Neuroscience

FMRP regulates tangential neuronal migration via MAP1B

Salima Messaoudi, Ada Allam, Julie Stoufflet, Théo Paillard, Coralie Fouquet, Mohamed Doulazmi, Anaïs Le Ven, Alain Trembleau, Isabelle Caillé

Sorbonne Université, CNRS UMR8246, Inserm U1130, Institut de Biologie Paris Seine(IBPS), Neuroscience Paris Seine (NPS), Paris, France • Laboratory of Molecular Regulation of Neurogenesis, GIGA-Stem Cells and GIGA-Neurosciences, University of Liège, CHU Sart Tilman, 4000 Liège, Belgium • Institut Curie, Paris, France • Université de Paris, Paris, France

Reviewed Preprint

Revised by authors after peer review.

About eLife's process

Reviewed preprint version 2
March 4, 2024 (this version)

Reviewed preprint version 1
July 5, 2023

Sent for peer review
May 11, 2023

Posted to preprint server
April 19, 2023

Abstract

The Fragile X Syndrome (FXS) represents the most prevalent form of inherited intellectual disability and is the first monogenic cause of Autism Spectrum Disorder. FXS results from the absence of the RNA-binding protein FMRP (Fragile X Messenger Ribonucleoprotein).

Neuronal migration is an essential step of brain development allowing displacement of neurons from their germinal niches to their final integration site. The precise role of FMRP in neuronal migration remains largely unexplored.

Using live imaging of postnatal Rostral Migratory Stream (RMS) neurons in Fmr1-null mice, we observed that the absence of FMRP leads to delayed neuronal migration and altered trajectory, associated with defects of centrosomal movement. RNA-interference-induced knockdown of *Fmr1* shows that these migratory defects are cell-autonomous. Notably, the primary FMRP mRNA target implicated in these migratory defects is MAP1B (Microtubule-Associated Protein 1B). Knocking-down MAP1B expression effectively rescued most of the observed migratory defects. Finally, we elucidate the molecular mechanisms at play by demonstrating that the absence of FMRP induces defects in the cage of microtubules surrounding the nucleus of migrating neurons, which is rescued by MAP1B knockdown.

Our findings reveal a novel neurodevelopmental role for FMRP in collaboration with MAP1B, jointly orchestrating neuronal migration by influencing the microtubular cytoskeleton.

eLife assessment

This study addresses the role of FMRP in the migration of newborn neuroblasts in the postnatal brain. Through extensive and **convincing** analysis of living imaging videos, the authors showed that neurons with FMRP deletion migrate aberrantly and exhibit defects in nucleokinesis and centrokinesis. The study presents a **valuable** finding on the mechanism of neuroblast migration in the postnatal brain.

Introduction

The Fragile X syndrome (FXS) is the most common cause of inherited intellectual disability and a leading cause of autism spectrum disorder. FXS is due to the silencing of the gene *FMR1* and loss of the encoded protein, FMRP (Fragile X Messenger Ribonucleoprotein) (Davis and Broadie, 2017). FMRP is an ubiquitous RNA-binding protein, with high level of expression in the central nervous system (Gholizadeh et al., 2015). It is a general regulator of RNA metabolism and especially of mRNA local translation in neurons (Banerjee et al., 2018). Its cognate mRNA targets are numerous and diverse, including mRNAs encoding proteins involved in neuronal plasticity like CamKIIα (Calcium Calmodulin-dependent Kinase II) and cytoskeletal proteins like MAP1B (Microtubule-Associated Protein 1B) (Ascano et al., 2012)(Brown et al., 2001)(Darnell et al., 2001)(Maurin et al., 2018). *Fmr1*-null mice are the murine model of FXS and have allowed characterization of numerous neurodevelopmental and plasticity defects consecutive to the absence of FMRP. We previously showed the essential role of FMRP in the differentiation and learning-induced structural plasticity of adult-generated olfactory bulb interneurons (Scotto-Lomassese et al., 2011)(Daroles et al., 2016).

Neuronal migration is a crucial step for the establishment of neuronal circuitry, orchestrating the relocation of neurons from their birthplace to their final destination for differentiation. Migration defects lead to severe brain pathologies including lissencephaly and cortical heterotopia and may contribute to psychiatric disorders (Romero et al., 2018). Interestingly, migration in the human infant brain appears to be even more extended than anticipated from the rodent data (Sanai et al., 2011)(Paredes et al., 2016). In addition, periventricular heterotopia has been documented in two individuals with FXS, implying a potential role for FMRP in migration (Moro et al., 2006). Importantly, in *Fmr1*-null mice, radially migrating embryonic glutamatergic cortical neurons display a defect in the multipolar to bipolar transition (La Fata et al., 2014), a critical change of polarity taking place before the initiation of the movement. The key FMRP mRNA involved in this process is N-Cadherin, down-regulated in the Fmr1 mutants and whose overexpression rescued the migratory phenotype. Additionally, both FMRP overexpression or knockdown lead to the misplacement of cortical glutamatergic neurons, also potentially underscoring its role in radial embryonic migration (Wu et al., 2019). However, to our knowledge, tangential neuronal migration in the absence of FMRP has not been studied so far and the dynamics of mutated *Fmr1* neurons have yet to be comprehensively analyzed.

Here, using the postnatal Rostral Migratory Stream (RMS) as a tangential migration model as in (Stoufflet et al., 2020), we present novel insights into the migratory defects induced by the absence of FMRP. Migrating neurons in Fmr1-null mice exhibit a distinctive pattern of slowed-down and erratic migration, accompanied by alterations of centrosome movement. Notably, these defects are cell-autonomous, as evidenced by their recapitulation through RNA-interference-induced Fmr1 knockdown (KD).

MAP1B (Microtubule Associated Protein 1B) is a microtubule-associated protein that plays a crucial role in the regulation of cytoskeletal dynamics within neurons. It is instrumental in brain development (Villarroel-Campos and Gonzalez-Billault, 2014) including neuronal migration (Yang et al., 2012)(González-Billault et al., 2005)(Gonzalez-Billault et al., 2004). We hypothesized its involvement as the FMRP mRNA target in the observed defects. Indeed, elevated levels of MAP1B were detected in the mutated RMS, and the knock-down induced downregulation of MAP1B successfully rescued most migration defects. Finally, we elucidate the molecular mechanisms underlying these migratory defects, by showing that the microtubular cage surrounding the nucleus of migrating neurons is disrupted in the absence of FMRP. Importantly, this abnormality is rescued by MAP1B KD, shedding light on a previously undiscovered role for the FMRP/MAP1B duo in regulating proper tangential migration at the microtubular level.

Results

FMRP is expressed in migrating neurons of the postnatal RMS

A massive number of neuroblasts are constantly produced in the ventricular/subventricular zone (V/SVZ) and migrate over a long distance along the RMS to the olfactory bulb (OB) (Lim and Alvarez-Buylla, 2016)(**Fig. 1A**). They display a cyclic saltatory mode of migration, in which the nucleus and centrosome move forward in a "two-stroke" cycle (Bellion et al., 2005). The centrosome moves first within a swelling in the leading process, termed here centrokinesis (CK) followed by movement of the nucleus, referred to as nucleokinesis (NK) (**Fig. 1B**). The neurons then pause and the cycle can reinitiate. After an *in vivo* intraventricular electroporation of a GFP-expressing plasmid in neonate mice, a sub-population of GFP-positive neurons can be visualized in the RMS a few days later (**Fig. 1C**).

FMRP is expressed in most neurons of the brain (Gholizadeh et al., 2015). Accordingly, immunostaining for FMRP reveals that FMRP is strongly expressed in the RMS, where most neurons appear labeled (**Fig. 1D**). In individual GFP-positive neurons, FMRP labeling appears as a discrete and punctate staining visible mainly in the cytoplasm both at the rear of the neuron and in the leading process (**Fig. 1E**). In order to more precisely localize FMRP at the subcellular level in migrating neurons, we performed culture of V/SVZ explants in Matrigel as described (Wichterle et al., 1997) followed by FMRP immunostaining (**Fig. 1F**). FMRP labeling appeared as a granular staining similarly visible around the nucleus, in the swelling and in the leading process.

FMRP cell-autonomously regulates neuronal migration

To investigate the involvement of FMRP in RMS migration, we used the *Fmr1-null* mouse line ("Fmr1 knockout mice," 1994). Time-lapse imaging of GFP positive neurons was performed in the control and *Fmr1-null* RMS (Movie S1, movie S2).

Fmr1-null neurons display a slowed-down migration, an increased pausing time, a more sinuous trajectory, and a defective directionality (**Fig. 2**.A-D). Additionally, the NK is less frequent and the mean distance per NK is reduced (**Fig. 2**.E,F).

Given the crucial role of the centrosome in neuronal migration (Higginbotham and Gleeson, 2007), we analyzed its dynamics by performing co-electroporation of GFP and Centrine-RFP in *Fmr1-null* and control neonate mice in order to co-label migrating neurons and their centrosome (Movie S3). The CK is slowed-down and less frequent in *Fmr1-null* neurons, as compared to controls (**Fig. 3**.A,B). A CK leading to a subsequent NK was defined as an efficient CK, as opposed to a CK not leading to an NK. CK efficiency is reduced in *Fmr1-null* neurons as compared to controls (**Fig. 3**.C).

To determine whether the observed migration defects are cell autonomous, we designed an interfering RNA coupled to GFP to cell-autonomously knock-down *Fmr1* mRNA in RMS neurons, similar to (Scotto-Lomassese et al., 2011). Its efficiency was assessed by FMRP immunostaining on electroporated SVZ explants in Matrigel. While all neurons electroporated by the control miRNeg-GFP were FMRP immunoreactive, this was reduced to 36% in miRFmr1-GFP electroporated neurons (Chi2 test, p-value = 0.01; miRNeg condition: N = 3, n = 15; miRFmr1 condition: N = 3, n = 14). The interfering mi*Fmr1*-GFP was thus co-electroporated with centrin-RFP to perform live-imaging. Analysis of migration and centrosome dynamics (Fig. S1 and S2) showed that *Fmr1* KD is sufficient to mostly recapitulate the migratory phenotype described in *Fmr1-null* mutants, revealing that FMRP cell-autonomously regulates neuronal migration (Kruskal Wallis followed by Dunn's post hoc analysis on the four genotypes). The only discernible difference lies in the directionality parameter, where defects are exacerbated in knockdown neurons compared to Fmr1-null mutants (Fisher test $p < 0.001$). This suggests that this defect might not be cell-autonomous in *Fmr1-null* mutants but rather a consequence of the mutated environment. This

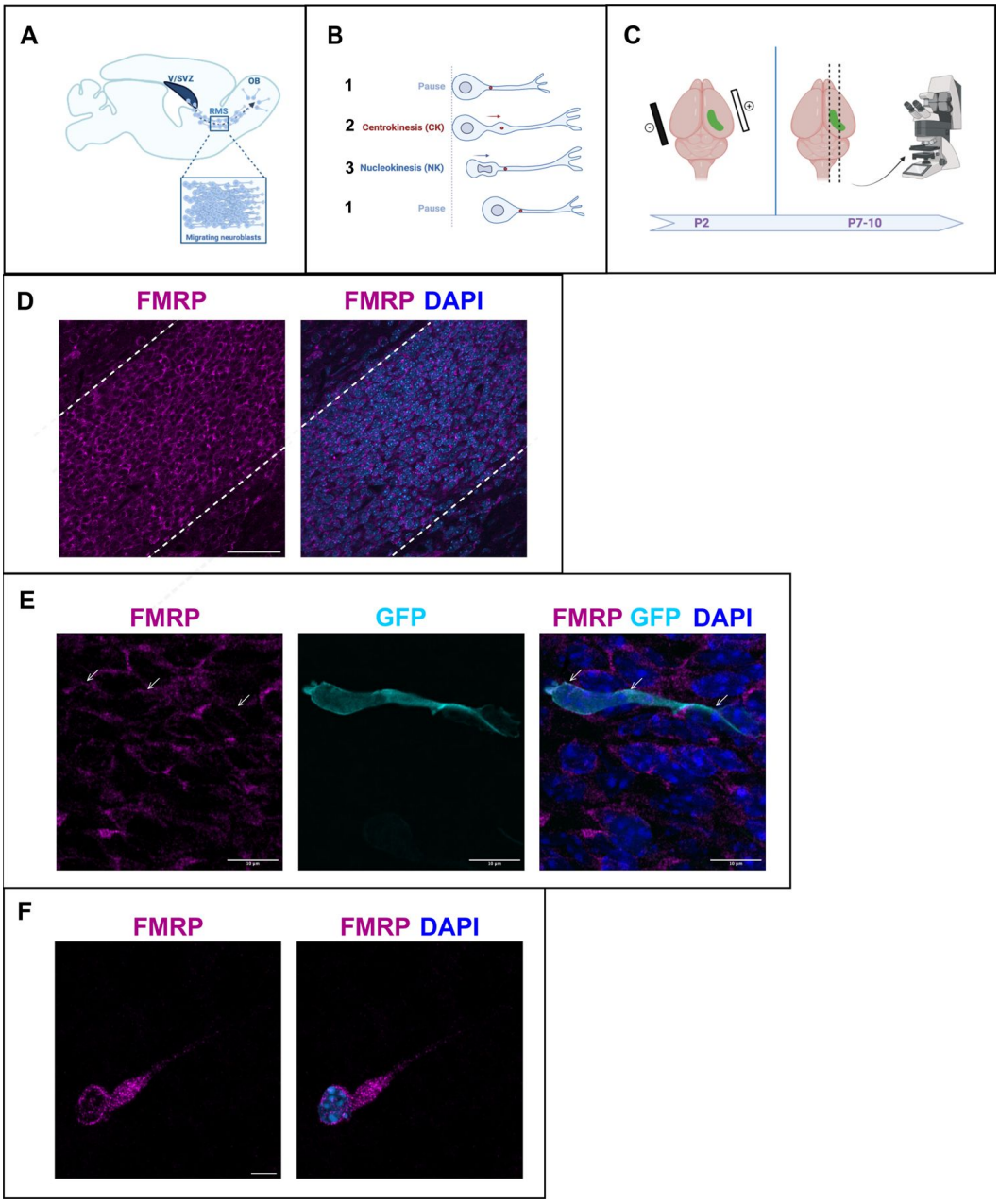

FIGURE 1.

FMRP is expressed in migrating neurons of the murine postnatal RMS.

(A) Scheme of a sagittal section of the postnatal RMS connecting the V/SVZ to the OB. V/SVZ, ventricular/sub-ventricular zone; OB, olfactory bulb; RMS, rostral migratory stream. The inset shows the high density of homotypically migrating neurons in the RMS. (B) Representation of cyclic saltatory migration. 1. The neuron is in pause. 2. The leading process extends, and the centrosome moves within a swelling in the leading process. 3. The nucleus moves forward. CK, centrokinesis; NK, nucleokinesis. (C) Scheme of the experimental procedure. 2-day old neonates are intraventricularly electroporated with a GFP-expressing plasmid to label a cohort of migrating neurons that can be subsequently visualized in fixed or acute sections of the RMS. (D) Immunohistochemistry of the RMS showing FMRP expression (magenta) along the stream. The RMS is delineated with dotted lines. Scale bar: 50 µm. (E) Immunohistochemistry of a GFP-positive RMS neuron (cyan) showing FMRP subcellular expression (magenta). The GFP-positive neuron displays a cytoplasmic expression of FMRP around the nucleus (indicated by white arrows). The surrounding GFP-negative neurons express FMRP as well, following the same pattern. Scale bar: 10 µm. (F) Immunostaining for FMRP of a neuroblast migrating away from a V/SVZ explant in Matrigel. The labeling appears granular in the cytoplasm around the nucleus, in the swelling and the leading process. Scale bar: 5 µm.

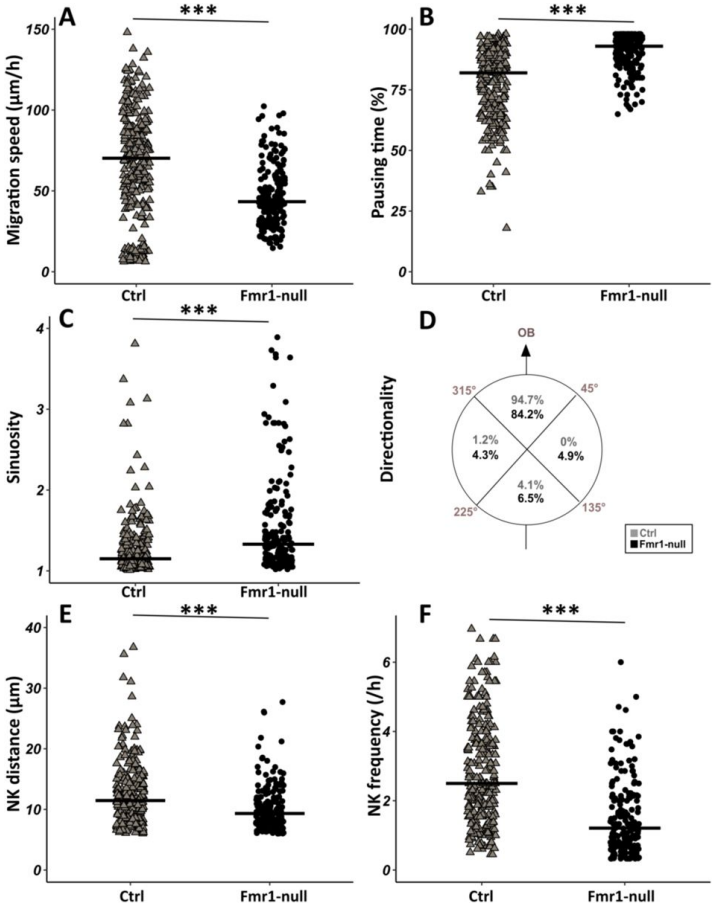

FIGURE 2.

Migration defects in Fmr1-null neurons.

(A) Migration speed of control (Ctrl) and Fmr1-null neurons. Ctrl: 70.62 (43.32) µm/h; Fmr1-null: 43.34 (25.97) µm/h (Kruskall-Wallis Test: Chi2 = 91.92, p-value < 0.001, df = 3; followed by Dunn's posthoc test). (B) Percentage of pausing time of control and Fmr1-null neurons. Ctrl: 82 (21.50); Fmr1-null: 93 (9.25) (Kruskall-Wallis Test: Chi2 = 130.61, p-value < 0.001, df = 3; followed by Dunn's posthoc test). (C) Sinuosity index of control and Fmr1-null neurons. Ctrl: 1.15 (0.26); Fmr1-null: 1.35 (0.66) (Kruskall-Wallis Test: Chi2 = 65.19, p-value < 0.001, df = 3; followed by Dunn's posthoc test). (D) Migration directionality radar represented in four spatial dials. Percentage of cells migrating in each spatial direction in control and Fmr1-null neurons, relatively to the vector going straight from the SVZ to the OB. (Fisher's Exact test, p-value < 0.001). (E) NK mean distance of control and Fmr1-null neurons. Ctrl: 11.46 (6.27) µm; Fmr1-null: 9.34 (4.16) µm (Kruskall-Wallis Test: Chi2 = 53.45, p-value < 0.001, df = 3; followed by Dunn's posthoc test). (F) NK frequency of control and Fmr1-null neurons. Ctrl: 2.5 (2.23) NK/h; Fmr1-null: 1.21 (1.45) NK/h (Kruskall-Wallis Test: Chi2 = 111.53, p-value < 0.001, df = 3; followed by Dunn's posthoc test). The black line represents the median. Ctrl: N = 3, n = 275; Fmr1-null: N = 3, n = 184. Median (IQR).***p-value < 0.001.

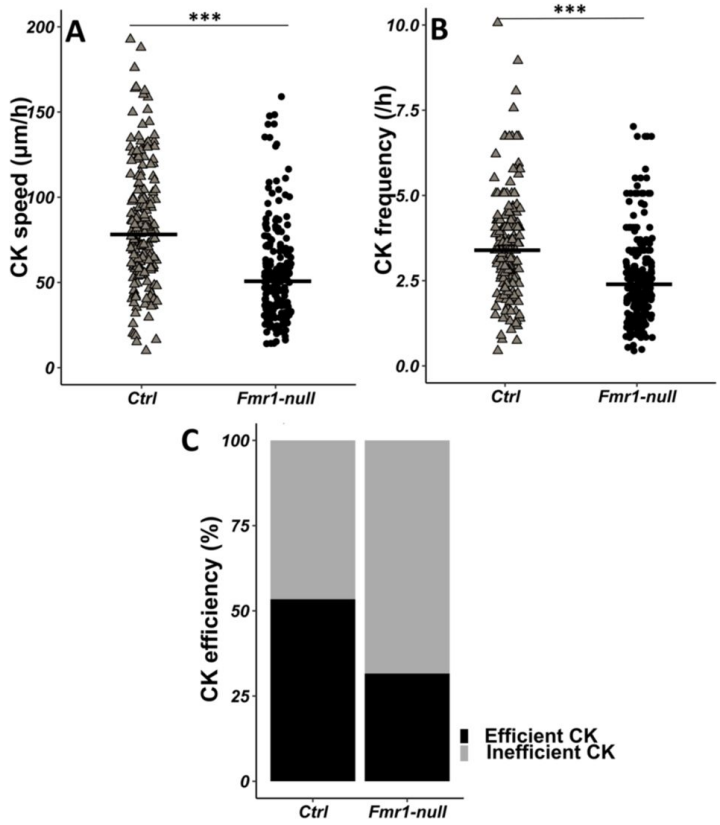

FIGURE 3.

CK defects in Fmr1-null neurons.

(A) CK speed of control and Fmr1-null neurons. Ctrl: 76.90 (46.46) µm/h; Fmr1-null: 49.45 (33.66) µm/h (Mann-Whitney test, p-value < 0.001). (B) CK frequency of control and Fmr1-null neurons. Ctrl: 3.33 (1.71) CK/h; Fmr1-null: 2.33 (1.71) CK/h (Mann-Whitney test, p-value < 0.001). (C) Percentage of efficient CKs in control and Fmr1-null neurons. Ctrl: 54 %; Fmr1-null: 33 % (Chi2 = 57.611, p-value < 0.001). The black line represents the median. Ctrl: N = 3, n = 178; Fmr1-null: N = 3, n = 216. Median (IQR). *** p-value < 0.001.

more pronounced directionality defect in the KD could be indicative of a lack of compensation in the acute KD context. Together, these data demonstrate that FMRP is cell-autonomously necessary for the proper neuronal migration of RMS neurons.

FMRP regulates neuronal migration through MAP1B

MAP1B is a neuron-specific microtubule-associated protein widely expressed in the developing CNS with crucial roles in diverse steps of neural development including neuronal migration (Yang et al., 2012)(González-Billault et al., 2005)(Gonzalez-Billault et al., 2004).

Immunostaining of the RMS revealed MAP1B expression, with most neurons appearing labeled (**Fig. 4A**). MAP1B subcellular staining is consistent with labeling of microtubules both around the nucleus and in the leading process (**Fig. 4B**). Immunostaining of individualized neurons migrating in Matrigel similarly showed a labeling around the nucleus and in the leading process, with occasional microtubule bundles (**Fig. 4C**).

MAP1B is a well-described FMRP mRNA target (Zhang et al., 2001)(Darnell et al., 2001)(Brown et al., 2001). Given its expression in RMS migrating neurons, it emerged as an interesting target for further investigation. As FMRP is a repressor of MAP1B mRNA translation (Brown et al., 2001)(Darnell et al., 2001)(Lu et al., 2004), the overall level of MAP1B typically appears increased in an *Fmr1-null* context (Lu et al., 2004)(Hou et al., 2006). Accordingly, the quantification of three independent Western Blots showed that MAP1B expression is increased on average by 1.6X in the RMS of *Fmr1-null* mice compared to controls (Fig. S4).

To investigate whether the observed migratory phenotype in *Fmr1-null* neurons is influenced by the upregulation of MAP1B, we cell-autonomously knocked-down *Map1b* in RMS neurons with an interfering RNA. Its efficiency was assessed by MAP1B immunostaining on electroporated SVZ explants in Matrigel, similar to the miRFmr1-GFP. While all neurons electroporated by the control miRNeg-GFP were MAP1B immunoreactive, this was reduced to 46 % in miRMAP1B-GFP electroporated neurons (Chi2 test, p-value < 0.001. miRNeg condition: N = 4, n =103; miRMap1b condition: N = 3, n = 113). The miR*Map1b*-GFP plasmid was electroporated in *Fmr1-null* neonate mice and time-lapse imaging was conducted on acute sections of the RMS (Movie S4). *Fmr1-null* neurons expressing miR*Map1b*-GFP exhibited a complete restoration of migration speed, pausing time, NK distance and frequency, making them comparable to miRNeg-GFP control neurons (**Fig. 5**.A,B,D,E). Notably, the sinuosity of *Fmr1-null* neurons expressing miR*Map1b*-GFP was not rescued (**Fig. 5C**), suggesting that this parameter is MAP1B-independent.

In conclusion, our results demonstrate that MAP1B is the primary FMRP mRNA target responsible for regulating neuronal migration.

The FMRP/MAP1B duo acts on the microtubular cage of RMS neurons

Considering the microtubule-associated functions of MAP1B, we investigated whether the migratory phenotype observed in Fmr1 mutants could be linked to a compromised microtubular cytoskeleton. To test this, we employed intraventricular electroporation of a plasmid expressing Doublecortin (DCX) fused to RFP for labeling the microtubules of Rostral Migratory Stream (RMS) neurons (Koizumi et al., 2006).

In control neurons co-electroporated with mirNeg-GFP, subsequent immunostaining revealed a well-defined cage of DCX-positive microtubule bundles smoothly encircling the nucleus in the vast majority of neurons, consistent with observations in other systems (**Fig. 6A**)(Rivas and Hatten, 1995)(Shu et al., 2004)(Xie et al., 2003). Contrastingly, mirFmr1-GFP coelectroporation with DCX-RFP unveiled an aberrant microtubular cage in a majority of neurons (**Fig. 6B**). These disorganized neurons exhibited disruptions in the cage (46% of them) or sinuous cages (33%) and

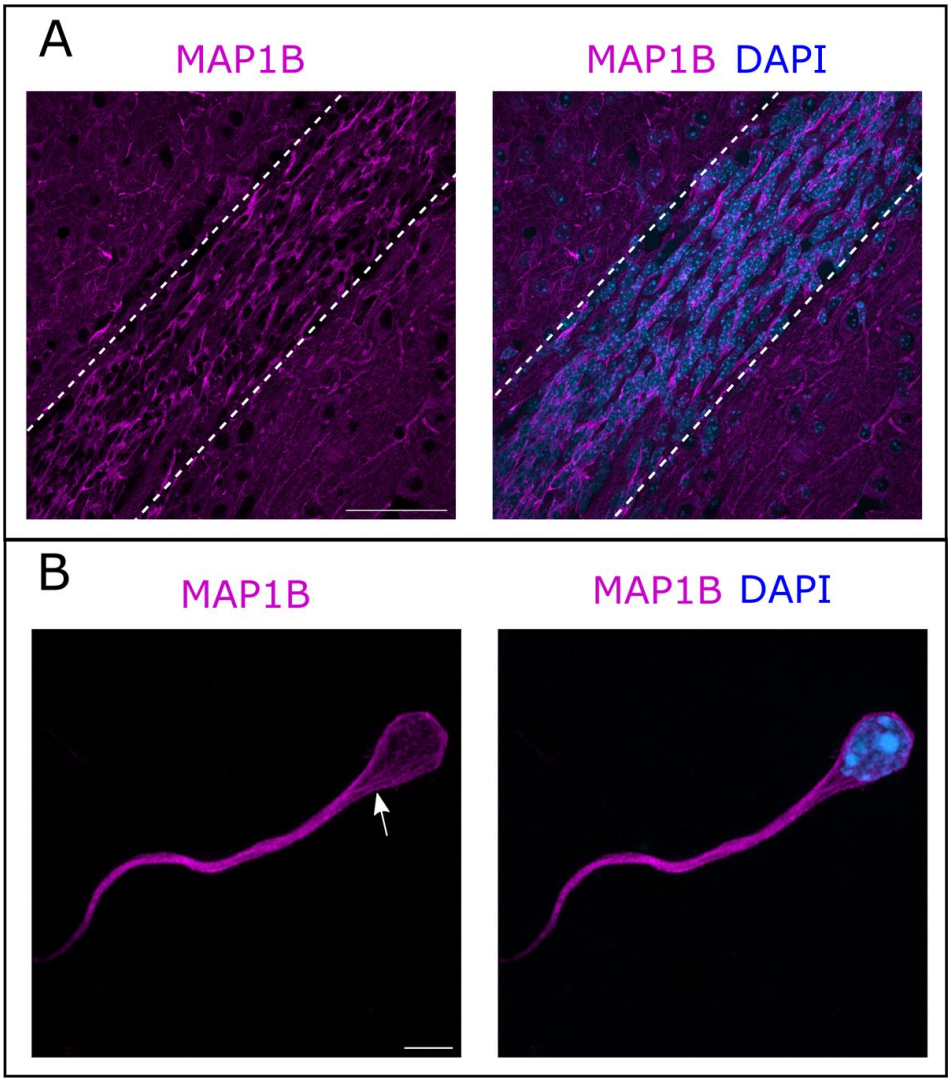

FIGURE 4.

MAP1B expression in the RMS.

(A) Immunohistochemistry of the RMS showing MAP1B expression (magenta) along the stream. The RMS is delineated with dotted lines. Scale bar: 50 μm. (B) Immunostaining for MAP1B of a neuroblast migrating away from a V/SVZ explant in Matrigel. The labeling is located around the nucleus and in the leading process with occasional bundles of potential microtubules (arrow). Scale bar: 5 μm.

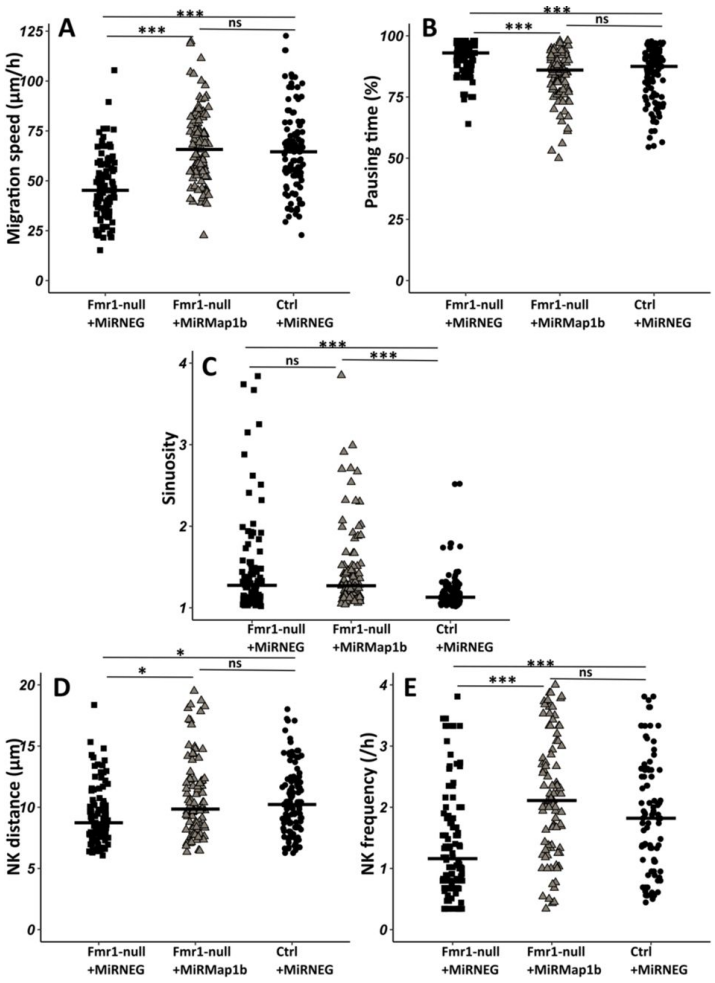

FIGURE 5.

Map1b KD rescues Fmr1-null neurons migration defects.

(A) Migration speed of Fmr1-null neurons expressing MiRNEG and MiRMap1b and control neurons expressing MiRNEG. Fmr1-null neurons + MiRNEG: 45.23 (23.25) µm/h; Fmr1-null neurons + MiRMap1b: 65.72 (24.31) µm/h; control neurons + MiRNEG: 64.54 (21.99) µm/h (Kruskall-Wallis Test: Chi2 = 61.168, p-value < 0.001, df = 2; followed by Dunn's posthoc test). (B) Percentage of pausing time of Fmr1-null neurons expressing MiRNEG and MiRMap1b and control neurons expressing MiRNEG. Fmr1-null neurons + MiRNEG: 93 (7); Fmr1-null neurons + MiRMap1b: 86 (14); control neurons + MiRNEG: 87.50 (15.67) (Kruskall-Wallis Test: Chi2 = 45.716, p-value < 0.001, df = 2; followed by Dunn's posthoc test). (C) Sinuosity index of Fmr1-null neurons expressing MiRNEG and MiRMap1b and control neurons expressing MiRNEG. Fmr1-null neurons + MiRNEG: 1.30 (0.45); Fmr1-null neurons + MiRMap1b: 1.28 (0.55); control neurons + MiRNEG: 1.13 (0.16) (Kruskall-Wallis Test: Chi2 = 39.807, p-value < 0.001, df = 2; followed by Dunn's posthoc test). (D) NK mean distance of Fmr1-null neurons expressing MiRNEG and MiRMap1b and control neurons expressing MiRNEG. Fmr1-null neurons + MiRNEG: 8.93 (3.64) µm; Fmr1-null neurons + MiRMap1b: 9.89 (3.85) µm; control neurons + MiRNEG: 10.23 (3.9) µm (Kruskall-Wallis Test: Chi2 = 11.573, p-value = 0.003, df = 2; followed by Dunn's posthoc test). (E) NK frequency of Fmr1-null neurons expressing MiRNEG and MiRMap1b and control neurons expressing MiRNEG. Fmr1-null neurons + MiRNEG: 1.18 (1.11)NK/h; Fmr1-null neurons + MiRMap1b:: 2.22(1.95)NK/h; control neurons + MiRNEG1.65(2) NK/h (Kruskall-Wallis Test: Chi2 = 39.272, p-value < 0.001, df = 2; followed by Dunn's posthoc test). The black line represents the median. Fmr1-null neurons + MiRNEG: N = 6, n = 102; Fmr1-null neurons + MiRMap1b: N = 3, n = 101; control neurons + MiRNEG: N = 3, n = 78. Median (IQR). * p-value < 0.05; *** p-value < 0.001; n.s.

sometimes even bundles of microtubules detaching from the nucleus (21%). Prompted by these findings, we investigated whether MAP1B overexpression in Fmr1 mutants was responsible for this microtubular aberration. Co-electroporation of DCX-RFP with mirFmr1-GFP and mirMAP1B-GFP indeed demonstrated a rescue of the abnormal cage in these double mutants (**Fig. 6C**, quantification in 6D).

In conclusion, our findings uncover the migratory phenotype of Fmr1 mutants, attributing it to an anomalous microtubular cage caused by MAP1B overexpression, elucidating a critical interplay between FMRP, MAP1B, and the microtubular cytoskeleton.

Discussion

FMRP is commonly described as a pivotal regulator of neuronal plasticity and neural development (Richter and Zhao, 2021). However, its role in neuronal migration remains poorly understood.

A role for FMRP in radial embryonic migration was first evidenced by (La Fata et al., 2014). This study revealed a misplacement of neurons in the embryonic cortical plate in *Fmr1-null* mutants, attributable to disruptions in the multipolar to bipolar transition, a step preceding the main movement of neurons. N-Cadherin emerged as the main FMRP target in this context. It is noteworthy that, while the study did not strongly indicate an impact on radial locomotion per se, drawing conclusive results is challenging due to the relatively low number of analyzed neurons. Subsequently, another study, focusing on miR-129, showed that *Fmr1* knock-down similarly triggered a misplacement of neurons in the cortical plate. However, this study did not display any further detailed analysis of the precise impact of *Fmr1* knock-down on radial migration (Wu et al., 2019). Furthermore, to our knowledge, there has been no exploration of tangential migration in the absence of FMRP, and the impact of its absence on the dynamics of saltatory migration remains unexplored.

We report here significant defects in postnatal tangential migration, characterized by a slowed-down and erratic trajectory. Notably, despite the mutated neurons experiencing delays and challenges in orienting themselves, they eventually reach the olfactory bulb (OB) correctly, as we previously demonstrated in the adult (Scotto-Lomassese et al., 2011). Importantly, while a delay in migration may not necessarily trigger important anatomical anomalies, when abnormally migrating neurons ultimately properly reach their target, it is noteworthy that a delay in the timing of differentiation of delayed neurons can lead to significant functional consequences (Bocchi et al., 2017).

Live imaging enabled us to conduct a detailed analysis of both nucleokinesis and centrosome dynamics, revealing profound perturbations in both processes. Given the crucial role of microtubules in regulating these processes (Kuijpers and Hoogenraad, 2011) (Tsai and Gleeson, 2005), our attention turned to MAP1B as the potential key FMRP mRNA target responsible for the observed migratory phenotypes. MAP1B is among the well-established targets of FMRP (Brown et al., 2001)(Darnell et al., 2001)(Zhang et al., 2001). As a neuron-specific microtubule-associated protein, MAP1B is expressed early in the embryonic brain (Tucker et al., 1989) and plays a crucial role in various stages of neural development (Gonzalez-Billault et al., 2004) including migration. MAP1B deficient mice display migration anomalies in the cortex, hippocampus and cerebellum and MAP1B phosphorylation can be induced by Reelin, a key regulator of radial migration (González-Billault et al., 2005).

We show MAP1B overexpression in *Fmr1*-mutated neurons and rescue the migratory defects through RNA-interference-induced KD. This establishes MAP1B as the critical FMRP mRNA target involved regulating cyclic saltatory migration. The significance of FMRP-regulated MAP1B translation was initially evidenced in *drosophila*, where it appeared essential for proper

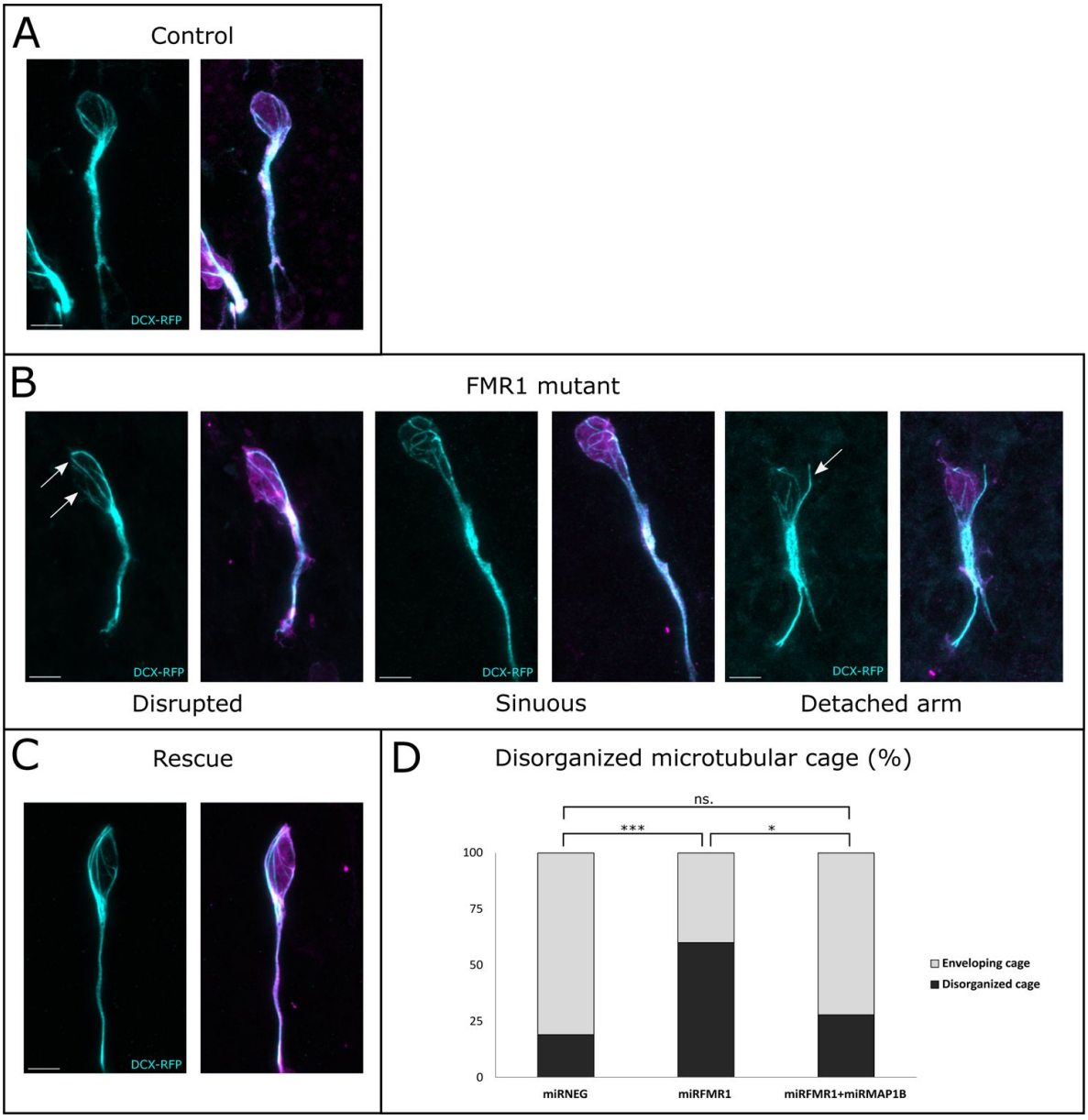

FIGURE 6.

The FMRP/MAP1B duo acts on the microtubular nuclear cage of RMS neurons.

(A) Representative control neurons from MirNeg-GFP (magenta) plus Dcx-RFP (cyan) cp-electroporated V/SVZ explants cultured in Matrigel displaying microtubular bundles enveloping the nucleus. (B) Representative Fmr1 KD neurons from MirFmr1-GFP (magenta) plus Dcx-RFP (cyan) co-electroporated V/SVZ explants cultured in Matrigel. The majority of them display an abnormal cage with disruption (arrows) (46%), sinuous cages (33% or even detached bundle (arrow) (28%). (C) Representative rescued neurons from MirNeg-GFP (magenta) plus Dcx-RFP (cyan) plus MirMAP1B co-electroporated V/SVZ explants cultured in Matrigel displaying microtubular bundles enveloping the nucleus. Scale bars: 5 µm. (D) Quantification of the percentage of disorganized cages in the different conditions: MirNeg 19%, miRFmr1 60%, mirFmr1 + mirMAP1B 28% (Pearson's χ^2 test (2, N=107)= 14.16, p-value < 0.001 with the Benjamini-Hochberg method for correcting multiple testing. MirNeg, N=3, n=37; MirFmr1 N=3, n=35; MirFmr1+MirMAP1B, n=36).

synaptogenesis (Zhang et al., 2001). This finding was subsequently confirmed in the mouse hippocampus, where elevated MAP1B levels in the *Fmr1*-null context also led to defective synaptogenesis (Lu et al., 2004). To our knowledge, the importance of the FMRP-MAP1B duo for neuronal migration, as described here, stands as the only other documented neurodevelopmental function of FMRP-regulated MAP1B translation. Considering the previously reported role of MAP1B in radial migration (González-Billault et al., 2005), it is tempting to hypothesize that our findings may extend to this form of embryonic migration, with the duo also regulating its microtubular dynamic.

Remarkably, we also elucidate the mechanistic action of the FMRP/MAP1B duo on the microtubular cytoskeleton. In the absence of FMRP, the cage formed by microtubules around the nucleus of migrating neurons appears disorganized. This disorganization primarily results from MAP1B overexpression in the Fmr1 mutants, as evidenced by the rescue of the phenotype through MAP1B knockdown. Notably, this phenotype of cage disruption was already described in radially migrating neurons upon Lis1, Dynein and Ndel1 KD (Shu et al., 2004). The Dynein/Lis1/Nde1/Nedl1 complex is essential to neuronal migration, allowing proper traction of the centrosome and nucleus along microtubules (Tsai et al., 2007). Considering that MAP1B has also been reported to impact the interaction between Dynein and Lis1 (Jiménez-Mateos et al., 2005), it is tempting to speculate that MAP1B overexpression in *Fmr1* mutants destabilizes the Dynein/Lis1/Nde1/Nedl1 complex, influencing the link it creates between the nuclear envelope and microtubules (Gonçalves et al., 2020) necessary for proper forward traction.

In the context of FXS, it is noteworthy that recent studies have revealed that postnatal tangential migration in the infant human brain is even more extensive than in mice (Paredes et al., 2016) (Sanai et al., 2011). Analyzing migration in FXS human organoids or forthcoming assembloids (Levy and Pașca, 2023) will enable to test the conservation of the migratory phenotype observed as well as its molecular underpinnings.

In conclusion, our findings unveil a novel facet of FMRP, highlighting its role as a regulator of migration intricately linked to microtubules through MAP1B. This discovery expands our understanding of this multifaceted protein and sheds a new light on its functional repertoire.

Material and methods

Mouse lines

Mice were housed in a 12 hours light/dark cycle, in cages containing one or two females and one male. The postnatal mice were housed in their parents' cage. Animal care was conducted in accordance with standard ethical guidelines [National Institutes of Health (NIH) publication no. 85-23, revised 1985 and European Committee Guidelines on the Care and Use of Laboratory Animals 86/609/EEC]. The experiments were approved by the local ethics committee (Comité d'Ethique en Expérimentation Animale Charles Darwin C2EA-05 and the French Ministère de l'Education Nationale, de l'Enseignement Supérieur et de la Recherche APAFIS#13624-2018021915046521_v5). We strictly performed this approved procedure. The mice used were in a C57BL6-J background. *Fmr1-null* mice were genotyped according to the original protocol ("Fmr1 knockout mice," 1994).

MiRNA production

Silencing of *Fmr1* and *Map1b* has been performed using BLOCK-iT Pol II miR RNAi Expression Vector Kits (Invitrogen) and the RNAi Designer (Invitrogen). The sequences of the single-stranded oligos are:

Fmr1 Top: TGCTGTACAAATGCCTTGTAGAAAGCGTTTTGGCCAACTGACTGACGCTTTCTAA GGCATTTGTA,

Fmr1 Bottom: CCTGTACAAATGCCTTAGAAAGCGTCAGTCAGTGGCCAAAACGCTTTCTACAAG GCATTTGTAC,

Map1b Top: TGCTGTGTTGATGAAGTCTTGGAGATGTTTTGGCCACTGACTGACATCTCCAACT TCATCAACA,

Map1b Bottom: CCTGTGTTGATGAAGTTGGAGATGTCAGTCAGTGGCCAAAACATCTCCAAGACT TCATCAACAC.

The double-stranded oligos were inserted in a pcDNA 6.2-GW/EmGFP-miR. The resulting constructions were sequenced before use.

Plasmids

The plasmids used for that study, in addition to the Mir plasmids described above (Invitrogen Block it kit) were pCAGGS-GFP (gift from S. Garel) and pCMV-centrinRFP (Addgene #26753).

Postnatal electroporation

Postnatal injection and electroporation were performed at postnatal day 2 (P2). Postnatal mice were anesthetized by hypothermia. Pseudo-stereotaxic injection [from lambda medial-lateral (M/L): 0,9; anterior-posterior (A/P): 1,1; dorsal-ventral (D/V): 2] using a glass micropipette (Drummond Scientific Company, Wiretrol I, 5-000-1050) was performed, and 2ul of plasmid (between 5 and 8 µg/ml) was injected. Animals were subjected to 5 pulses of 99.9V during 50ms separated by 950ms using the CUY21 SC Electroporator and 10-mm tweezer electrodes (Harvard Apparatus, Tweezertrode, 10mm, 45-0119). The animals were placed on 37°C plates to restore their body temperature before returning in their parents' cage. Animals were considered as fully recovered when moving naturally and their skin color hadreturned to pink.

Postnatal acute brain slices

Brain slices of mice aged from P6 to P10 were prepared as previously described in (Stoufflet et al., 2020). Pups were sacrificed by decapitation and the brain was removed from the skull. Sagittal brain sections (250 µm) were cut with a VT1200S vibratome (Leica). Slices were prepared in an ice-cold cutting solution of the following composition: 125 mM NaCl, 0.4 mM $CaCl_2$, 1 mM $MgCl_2$, 1.25 mM NaH_2PO_4, 26 mM $NaHCO_3$, 5 mM sodium pyruvate, 20 mM glucose and 1 mM kynurenic acid, saturated with 5% CO_2 and 95% O_2. Slices were incubated in this solution for 30 minutes at room temperature and then placed in recording solution (identical to the cutting solution, except that the $CaCl_2$ concentration is 2 mM and kynurenic acid is absent) for at least 30 minutes at 32°C before image acquisition.

Time-lapse video microscopy of postnatal slices

To analyze neuronal migration and centrosome dynamics, images were obtained with an inverted SP5D confocal microscope (Leica) using a 40x/1.25-numerical aperture (N.A.) objective with 1.5 optical zoom or an upright SP5 MPII two-photon microscope (Leica) using a 25x/0.95-N.A. objective with 1.86 optical zoom. Images were acquired every 3 minutes for 2 to 3 hours. The temperature in the microscope chamber was maintained at 32°C during imaging and brain slices were continuously perfused with heated recording solution (see above) saturated with 5% CO_2 and 95% O_2.

Analyses of neuronal migration and centrosome movement

Analyses were performed using ImageJ (NIH Image; National Institutes of Health, Bethesda, MD) software and MTrackJ plugin. The nucleus and the centrosome (when centrin-RFP was co-injected) were tracked manually on each time frame during the whole movie. We considered a NK as a movement superior to 6 µm between two consecutive time points (3 minutes-interval). For cell migration, calculation of speed, percentage of pausing time, sinuosity, directionality, NK distance and frequency was performed using the x,y,t coordinates of the nucleus of each cell. Cells tracked for less than 30 minutes and cells that did not perform any NK during the whole tracking were excluded. A CK was defined as a forward movement superior to 2 µm followed by a backward movement superior to 2 µm. For centrosome movement, calculation of CK speed, frequency and efficiency was performed using the x,y,t coordinates of the centrosome of each cell and the x,y,t coordinates of each corresponding nucleus.

More specifically, speed was calculated by summing all the distances traveled by one cell and dividing the total distance by the total time, including time slots (3 minutes-interval) when the cell pauses.

The pausing time is calculated as the sum of the time slots during which the cell moves less than 6 µm, hence below the cut-off for a NK.

The sinuosity index is the ratio between the total distance covered by the cell and the euclidean distance between its starting and ending points.

The assessment of directionality involves calculating a migration angle (θ), defined as the angle between a neuron's vector from its starting point to its destination and a hypothetical vector connecting the subventricular zone (SVZ) to the olfactory bulb (OB). Migration angles range from 0° to 360°, with 0° representing precise alignment with the SVZ-to-OB direction. To simplify, we employ 'migration radars' to depict cell migration angles, segmented for visualizing the distribution of directions.

An efficient CK was defined as a forward movement of the centrosome greater than 2 µm followed by a backward movement greater than 2 µm, associated to a subsequent NK (movement of the nucleus greater than 6 µm). An inefficient CK was defined by the same centrosomal movement not followed by an NK.

Immunohistochemistry

P7 to P10 mice were lethally anesthetized using Euthasol. Intracardiac perfusion with 4% paraformaldehyde was performed. The brain was post-fixed overnight in 4% paraformaldehyde and then rinsed three times with phosphate-buffered saline (PBS) 1x (Gibco, 1400-067). 50 µm sagittal sections were made with VT1200S microtome (Leica). Slices were placed 1 hour in a saturation solution (10% fetal bovine serum; 0.5% Triton X-100 in PBS). Primary antibodies used in this study are: GFP (Aves; GFP-1020; 1/1000), FMRP (Developmental Studies Hybridoma Bank; 2F5-1; 1/200), MAP1B (Santa Cruz Biotechnology; sc-365668; 1/300). The antibodies were diluted in saturation solution. Slices were incubated for 48 to 72 hours at 4°C under agitation with the antibodies and then rinsed three times with PBS 1x. Secondary antibodies used are: anti-chicken immunoglobulin Y (IgY) Alexa Fluor 488 (1/1000; Jackson ImmunoResearch; 703-545-155) against anti-GFP, anti-mouse immunoglobulin G2b (IgG2b) Alexa Fluor 555 (1/2000; Jackson ImmunoResearch; 703-545-155) against anti-FMRP and anti-MAP1B. The antibodies were diluted in saturation solution. Slices were incubated with secondary antibodies for 1 hour at room temperature under agitation, protected from light. After rinsing three times with PBS 1x, slices were counter-colored with Hoechst and mounted in Mowiol.

Immunostaining on SVZ explants in Matrigel

For the quantification of mirFmr1 and miR*Map1b* efficiency, the SVZ of electroporated mice were dissected as described. SVZ explants were placed on glass-bottom culture dishes (MatTek Corporation; P35G-0-20-C) within 10 mL of 60% Matrigel (Corning; 356237). After Matrigel solidification (15 minutes at 37°C, 5% CO_2), culture medium was added and the dishes were incubated for 4-5 days at 37°C, 5% CO_2. For FMRP and MAP1B immunostaining, SVZ cultures were fixed in 2% paraformaldehyde for 30 minutes and then rinsed three times with PBS 1x. Immunostaining was then performed as for sections (see above). To quantify *Fmr1* and *Map1b* KD, a cell was considered MAP1B or FMRP negative when it was clearly immunonegative at high magnification.

Tissue collection and Western blotting

RMS were manually micro-dissected from 5 to 6 postnatal mouse brains and pooled in a PBS 1x (0.5% glucose) solution. After centrifugation, protein extraction was performed on the tissue pellet. Samples were homogenized in a lysis buffer 25 mM Tris HCl pH 7.5, 150 mM NaCl, 1% NP40, 0.5% NaDeoxycholate, 1 mM EDTA, 5% glycerol, 1X EDTA-free protease inhibitor cocktail (Sigma, 4693132001). After centrifugation, samples were loaded and run on NuPAGE 3-8% Tris-Acetate Gel (Invitrogen, EA0378BOX) at 120V for 15 minutes then 180V for 40 minutes. Transfer to nitrocellulose Immobilon-PVDF-P membrane (Millipore, IPVH00010) was performed at 40V overnight at 4°C. The membrane was then saturated for 1 hour in TBSt containing 5% powder milk. Primary antibodies used are: MAP1B (Santa Cruz Biotechnology, sc-365668, 1/100), Vinculin (Cell Signaling Technology, 13901S, 1/1000). The antibodies were diluted in TBSt containing 5% powder milk. Secondary antibodies used are: ECL anti-mouse immunoglobulin G (IgG) horseradish peroxidase linked whole antibody (1/10 000; Fisher Scientific; NXA931V) for anti-MAP1B, Peroxidase-conjuguated AffiniPure F(ab')2 Fragment Donkey Anti-Rabbit IgG (H+L) (1/5 000; Jackson ImmunoResearch; 711-036-152) for anti-Vinculin. The antibodies were diluted in TBSt containing 5% powder milk. Labeling was visualized using Pierce ECL Western Blotting Substrate (Thermo Scientific; 32209) and luminescent image analyzer LAS-3000.

Statistics

All manipulations and statistical analyses were implemented with R (4.2.1, R Foundation for Statistical Computing, Vienna, Austria). Normality in the variable distributions was assessed by the Shapiro-Wilk test. Furthermore, the Levene test was performed to probe homogeneity of variances across groups. Variables that failed the Shapiro-Wilk or the Levene test were analyzed with non-parametric statistics using the one-way Kruskal-Wallis analysis of variance on ranks followed by Dunn's posthoc test and Mann-Whitney rank sum tests for pairwise multiple comparisons. Variables that passed the normality test were analyzed by means of one-way ANOVA followed by Tukey post hoc test for multiple comparisons or by Student's *t* test for comparing two groups. Categorical variables were compared using Pearson's c^2 test or Fisher's exact test. A *p*- value of <0.05 was used as a cutoff for statistical significance. Results are presented as the median (interquartile range [IQR]). The statistical tests are described in each figure legend.

Fundings

This work was funded by Fondation Jérôme Lejeune, ANR NotifX ANR-20-CE16-0016 and NIH contract NIDCD Grant R01-DC-017989.

Acknowledgements

We thank Isabelle Dusart for expert reading as well as Caroline Dubacq and Oriane Trouillard for technical help. The experiments were performed in IBPS imaging facility and the mice were housed in IBPS animal facility.

FIGURE S1. Fmr1 KD recapitulates Fmr1-null neuronal migration defects. (A) Migration speed of neurons expressing MiRNEG and MiRFmr1. MiRNEG: 72.94 (36.67) µm/h; MiRFmr1: 48.8 (30.78)µm/h (Kruskall-Wallis Test: Chi2 = 91.92, p-value < 0.001, df = 3; followed by Dunn's posthoc test). (B) Percentage of pausing time of neurons expressing MiRNEG and MiRFmr1. MiRNEG: 80.62 (16.70); MiRFmr1: 92.31 (12.98) (Kruskall-Wallis Test: Chi2 = 130.61, p-value < 0.001, df = 3; followed by Dunn's posthoc test). (C) Sinuosity index of neurons expressing MiRNEG and MiRFmr1. MiRNEG: 1.20 (0.31); MiRFmr1: 1.36 (0.61) (Kruskall-Wallis Test: Chi2 = 65.19, p-value < 0.001, df = 3; followed by Dunn's posthoc test). (D) Migration directionality radar represented in four spatial dials. Percentage of cells migrating in each spatial direction in neurons expressing MiRNEG and MiRFmr1, relatively to the vector going straight from the SVZ to the OB. (Fisher's Exact test, p-value = 0.019). (E) NK mean distance of neurons expressing MiRNEG and MiRFmr1. MiRNEG: 12.34(5.65)µm; MiRFmr1: 9.16 (3.61) µm (Kruskall-Wallis Test: Chi2 = 53.45, p-value < 0.001, df = 3; followed by Dunn's posthoc test). (F) NK frequency of neurons expressing MiRNEG and MiRFmr1. MiRNEG: 2.55 (2.18)NK/ h; MiRFmr1: 1.48 (1.95) NK/h (Kruskall-Wallis Test: Chi2 = 111.53, p-value < 0.001, df = 3; followed by Dunn's posthoc test). The black line represents the median. MiRNEG: N = 3, n = 86; MiRFmr1: N = 3, n = 79. Median (IQR). * p-value < 0.05; ** p-value < 0.005; *** p-value < 0.001.

FIGURE S2. Fmr1 KD recapitulates Fmr1-null neurons CK defects. (A) CK speed of neurons expressing MiRNEG and MiRFmr1. MiRNEG: 89.71(55.06) µm/h; MiRFmr1: 64.72 (33.89) µm/h (Mann-Whitney test, p-value < 0.001). (B) CK frequency of neurons expressing MiRNEG and MiRFmr1. MiRNEG: 3.18 (1.50) CK/h; MiRFmr1: 2.50 (1.64)CK/h (Mann-Whitney test, p-value = 0.011). (C) Percentage of efficient CKs in neurons expressing MiRNEG and MiRFmr1. MiRNEG: 57 %; MiRFmr1: 41 % (Chi2 = 17.999, p-value = 0.0012). The black line represents the median. MiRNEG: N = 3, n = 96; MiRFmr1: N = 3, n = 81. Median (IQR). *p-value < 0.05; **p-value < 0.005; *** p-value < 0.001.

FIGURE S3. MAP1B is overexpressed in Fmr1-null RMS neurons. (A) Immunoblot analysis revealing the expression of MAP1B in control and Fmr1-null micro-dissected RMS. (B) Quantification of MAP1B signal was performed with NIH IMAGE software and normalized to Vinculin house-keeping gene signal. MAP1B level in Fmr1-null RMS was statistically compared and normalized to MAP1B level in control RMS. (Student's test, p-value = 0.004). (Ctrl: N = 3; MAP1B KD: N = 3. **p-value < 0.005.)

References

Ascano M *et al.* (2012) **FMRP targets distinct mRNA sequence elements to regulate protein expression** *Nature* **492**:382–386 https://doi.org/10.1038/nature11737

Banerjee A, Ifrim MF, Valdez AN, Raj N, Bassell GJ (2018) **Aberrant RNA translation in fragile X syndrome: From FMRP mechanisms to emerging therapeutic strategies** *Brain Res* **1693**:24–36 https://doi.org/10.1016/j.brainres.2018.04.008

Bellion A, Baudoin J-P, Alvarez C, Bornens M, Métin C (2005) **Nucleokinesis in Tangentially Migrating Neurons Comprises Two Alternating Phases: Forward Migration of the Golgi/Centrosome Associated with Centrosome Splitting and Myosin Contraction at the Rear** *J Neurosci* **25**:5691–5699 https://doi.org/10.1523/JNEUROSCI.1030-05.2005

Bocchi R, Egervari K, Carol-Perdiguer L, Viale B, Quairiaux C, De Roo M, Boitard M, Oskouie S, Salmon P, Kiss JZ. (2017) **Perturbed Wnt signaling leads to neuronal migration delay, altered interhemispheric connections and impaired social behavior** *Nat Commun* **8** https://doi.org/10.1038/s41467-017-01046-w

Brown V *et al.* (2001) **Microarray Identification of FMRP-Associated Brain mRNAs and Altered mRNA Translational Profiles in Fragile X Syndrome** *Cell* **107**:477–487 https://doi.org/10.1016/S0092-8674(01)00568-2

Darnell JC, Jensen KB, Jin P, Brown V, Warren ST, Darnell RB (2001) **Fragile X Mental Retardation Protein Targets G Quartet mRNAs Important for Neuronal Function** *Cell* **107**:489–499 https://doi.org/10.1016/S0092-8674(01)00566-9

Daroles L, Gribaudo S, Doulazmi M, Scotto-Lomassese S, Dubacq C, Mandairon N, Greer CA, Didier A, Trembleau A, Caillé I (2016) **Fragile X Mental Retardation Protein and Dendritic Local Translation of the Alpha Subunit of the Calcium/Calmodulin-Dependent Kinase II Messenger RNA Are Required for the Structural Plasticity Underlying Olfactory Learning** *Biological Psychiatry* **80**:149–159 https://doi.org/10.1016/j.biopsych.2015.07.023

Davis JK, Broadie K (2017) **Multifarious Functions of the Fragile X Mental Retardation Protein** *Trends in Genetics* **33**:703–714 https://doi.org/10.1016/j.tig.2017.07.008

Fmr1 knockout mice: a model to study fragile X mental retardation (1994) **The Dutch-Belgian Fragile X Consortium** *Cell* **78**:23–33

Gholizadeh S, Halder SK, Hampson DR (2015) **Expression of fragile X mental retardation protein in neurons and glia of the developing and adult mouse brain** *Brain Research* **1596**:22–30 https://doi.org/10.1016/j.brainres.2014.11.023

Gonçalves JC, Quintremil S, Yi J, Vallee RB (2020) **Nesprin-2 Recruitment of BicD2 to the Nuclear Envelope Controls Dynein/Kinesin-Mediated Neuronal Migration In Vivo** *Current Biology* **30**:3116–3129 https://doi.org/10.1016/j.cub.2020.05.091

González-Billault C *et al.* (2005) **A role of MAP1B in Reelin-dependent neuronal migration** *Cereb Cortex* **15**:1134–1145 https://doi.org/10.1093/cercor/bhh213

Gonzalez-Billault C, Jimenez-Mateos EM, Caceres A, Diaz-Nido J, Wandosell F, Avila J (2004) **Microtubule-associated protein 1B function during normal development, regeneration, and pathological conditions in the nervous system** *Journal of Neurobiology* **58**:48–59 https://doi.org/10.1002/neu.10283

Higginbotham HR, Gleeson JG (2007) **The centrosome in neuronal development** *Trends in Neurosciences* **30**:276–283 https://doi.org/10.1016/j.tins.2007.04.001

Hou L, Antion MD, Hu D, Spencer CM, Paylor R, Klann E (2006) **Dynamic translational and proteasomal regulation of fragile X mental retardation protein controls mGluR-dependent long-term depression** *Neuron* **51**:441–454 https://doi.org/10.1016/j.neuron.2006.07.005

Jiménez-Mateos EM, Wandosell F, Reiner O, Avila J, González-Billault C (2005) **Binding of microtubule-associated protein 1B to LIS1 affects the interaction between dynein and LIS1** *Biochem J* **389**:333–341 https://doi.org/10.1042/BJ20050244

Koizumi H, Higginbotham H, Poon T, Tanaka T, Brinkman BC, Gleeson JG (2006) **Doublecortin maintains bipolar shape and nuclear translocation during migration in the adult forebrain** *Nat Neurosci* **9**:779–786 https://doi.org/10.1038/nn1704

Kuijpers M, Hoogenraad CC (2011) **Centrosomes, microtubules and neuronal development. Molecular and Cellular Neuroscience** *Membrane Trafficking and Cytoskeletal Dynamics in Neuronal Function* **48**:349–358 https://doi.org/10.1016/j.mcn.2011.05.004

La Fata G *et al.* (2014) **FMRP regulates multipolar to bipolar transition affecting neuronal migration and cortical circuitry** *Nat Neurosci* **17**:1693–1700 https://doi.org/10.1038/nn.3870

Levy RJ, Paşca SP (2023) **What Have Organoids and Assembloids Taught Us About the Pathophysiology of Neuropsychiatric Disorders? Biological Psychiatry** *Neural Organoids to Study Psychiatric Disease: The Pros and Cons* **93**:632–641 https://doi.org/10.1016/j.biopsych.2022.11.017

Lim DA, Alvarez-Buylla A (2016) **The Adult Ventricular–Subventricular Zone (V-SVZ) and Olfactory Bulb (OB) Neurogenesis** *Cold Spring Harb Perspect Biol* **8** https://doi.org/10.1101/cshperspect.a018820

Lu R, Wang H, Liang Z, Ku L, O'donnell WT, Li W, Warren ST, Feng Y (2004) **The fragile X protein controls microtubule-associated protein 1B translation and microtubule stability in brain neuron development** *Proc Natl Acad Sci U S A* **101**:15201–15206 https://doi.org/10.1073/pnas.0404995101

Maurin T, Lebrigand K, Castagnola S, Paquet A, Jarjat M, Popa A, Grossi M, Rage F, Bardoni B (2018) **HITS-CLIP in various brain areas reveals new targets and new modalities of RNA binding by fragile X mental retardation protein** *Nucleic Acids Res* **46**:6344–6355 https://doi.org/10.1093/nar/gky267

Moro F *et al.* (2006) **Periventricular heterotopia in fragile X syndrome** *Neurology* **67**:713–715 https://doi.org/10.1212/01.wnl.0000230223.51595.99

Paredes MF *et al.* (2016) **Extensive migration of young neurons into the infant human frontal lobe** *Science* **354** https://doi.org/10.1126/science.aaf7073

Richter JD, Zhao X (2021) **The molecular biology of FMRP: new insights into fragile X syndrome** *Nat Rev Neurosci* **22**:209–222 https://doi.org/10.1038/s41583-021-00432-0

Rivas RJ, Hatten ME (1995) **Motility and cytoskeletal organization of migrating cerebellar granule neurons** *J Neurosci* **15**:981–989 https://doi.org/10.1523/JNEUROSCI.15-02-00981.1995

Romero DM, Bahi-Buisson N, Francis F (2018) **Genetics and mechanisms leading to human cortical malformations. Seminars in Cell & Developmental Biology** *Neocortical development* **76**:33–75 https://doi.org/10.1016/j.semcdb.2017.09.031

Sanai N *et al.* (2011) **Corridors of migrating neurons in the human brain and their decline during infancy** *Nature* **478**:382–386 https://doi.org/10.1038/nature10487

Scotto-Lomassese S, Nissant A, Mota T, Néant-Féry M, Oostra BA, Greer CA, Lledo P-M, Trembleau A, Caillé I (2011) **Fragile X Mental Retardation Protein Regulates New Neuron Differentiation in the Adult Olfactory Bulb** *J Neurosci* **31**:2205–2215 https://doi.org/10.1523/JNEUROSCI.5514-10.2011

Shu T, Ayala R, Nguyen M-D, Xie Z, Gleeson JG, Tsai L-H (2004) **Ndel1 Operates in a Common Pathway with LIS1 and Cytoplasmic Dynein to Regulate Cortical Neuronal Positioning** *Neuron* **44**:263–277 https://doi.org/10.1016/j.neuron.2004.09.030

Stoufflet J, Chaulet M, Doulazmi M, Fouquet C, Dubacq C, Métin C, Schneider-Maunoury S, Trembleau A, Vincent P, Caillé I (2020) **Primary cilium-dependent cAMP/PKA signaling at the centrosome regulates neuronal migration** *Science Advances* **6** https://doi.org/10.1126/sciadv.aba3992

Tsai J-W, Bremner KH, Vallee RB (2007) **Dual subcellular roles for LIS1 and dynein in radial neuronal migration in live brain tissue** *Nature Neuroscience* **10**:970–979 https://doi.org/10.1038/nn1934

Tsai L-H, Gleeson JG (2005) **Nucleokinesis in Neuronal Migration** *Neuron* **46**:383–388 https://doi.org/10.1016/j.neuron.2005.04.013

Tucker RP, Garner CC, Matus A (1989) **In situ localization of microtubule-associated protein mRNA in the developing and adult rat brain** *Neuron* **2**:1245–1256 https://doi.org/10.1016/0896-6273(89)90309-7

Villarroel-Campos D, Gonzalez-Billault C (2014) **The MAP1B case: An old MAP that is new again** *Developmental Neurobiology* **74**:953–971 https://doi.org/10.1002/dneu.22178

Wichterle H, García-Verdugo JM, Alvarez-Buylla A (1997) **Direct Evidence for Homotypic, Glia-Independent Neuronal Migration** *Neuron* **18**:779–791 https://doi.org/10.1016/S0896-6273(00)80317-7

Wu C *et al.* (2019) **MicroRNA-129 modulates neuronal migration by targeting Fmr1 in the developing mouse cortex** *Cell Death Dis* **10**:1–13 https://doi.org/10.1038/s41419-019-1517-1

Xie Z, Sanada K, Samuels BA, Shih H, Tsai L-H (2003) **Serine 732 Phosphorylation of FAK by Cdk5 Is Important for Microtubule Organization, Nuclear Movement, and Neuronal Migration** *Cell* **114**:469–482 https://doi.org/10.1016/S0092-8674(03)00605-6

Yang M, Wu M, Xia P, Wang C, Yan P, Gao Q, Liu J, Wang H, Duan X, Yang X (2012) **The role of microtubule-associated protein 1B in axonal growth and neuronal migration in the central nervous system** *Neural Regen Res* **7**:842–848 https://doi.org/10.3969/j.issn.1673-5374.2012.11.008

Zhang YQ, Bailey AM, Matthies HJG, Renden RB, Smith MA, Speese SD, Rubin GM, Broadie K (2001) **Drosophila Fragile X-Related Gene Regulates the MAP1B Homolog Futsch to Control Synaptic Structure and Function** *Cell* **107**:591–603 https://doi.org/10.1016/S0092-8674(01)00589-X

Article and author information

Salima Messaoudi
Sorbonne Université, CNRS UMR8246, Inserm U1130, Institut de Biologie Paris Seine(IBPS), Neuroscience Paris Seine (NPS), Paris, France

Ada Allam
Sorbonne Université, CNRS UMR8246, Inserm U1130, Institut de Biologie Paris Seine(IBPS), Neuroscience Paris Seine (NPS), Paris, France

Julie Stoufflet
Sorbonne Université, CNRS UMR8246, Inserm U1130, Institut de Biologie Paris Seine(IBPS), Neuroscience Paris Seine (NPS), Paris, France, Laboratory of Molecular Regulation of Neurogenesis, GIGA-Stem Cells and GIGA-Neurosciences, University of Liège, CHU Sart Tilman, 4000 Liège, Belgium

Théo Paillard
Sorbonne Université, CNRS UMR8246, Inserm U1130, Institut de Biologie Paris Seine(IBPS), Neuroscience Paris Seine (NPS), Paris, France

Coralie Fouquet
Sorbonne Université, CNRS UMR8246, Inserm U1130, Institut de Biologie Paris Seine(IBPS), Neuroscience Paris Seine (NPS), Paris, France

Mohamed Doulazmi
Sorbonne Université, CNRS UMR8246, Inserm U1130, Institut de Biologie Paris Seine(IBPS), Neuroscience Paris Seine (NPS), Paris, France

Anaïs Le Ven
Sorbonne Université, CNRS UMR8246, Inserm U1130, Institut de Biologie Paris Seine(IBPS), Neuroscience Paris Seine (NPS), Paris, France, Institut Curie, Paris, France

Alain Trembleau
Sorbonne Université, CNRS UMR8246, Inserm U1130, Institut de Biologie Paris Seine(IBPS), Neuroscience Paris Seine (NPS), Paris, France

Isabelle Caillé
Sorbonne Université, CNRS UMR8246, Inserm U1130, Institut de Biologie Paris Seine(IBPS), Neuroscience Paris Seine (NPS), Paris, France, Université de Paris, Paris, France
For correspondence: isabelle.caille@upmc.fr

Copyright

Editors

Reviewing Editor
Fadel Tissir
Université Catholique de Louvain, Brussels, Belgium

Senior Editor
Sofia Araújo
University of Barcelona, Barcelona, Spain

Reviewer #1 (Public Review):

This study investigated Fragile X Messenger Ribonucleoprotein (FMRP) protein impact on neuroblast tangential migration in the postnatal rostral migratory stream (RMS). Authors conducted a series of live-imaging on organotypic brain slices from Fmr1-null mice. They continued their analysis silencing Fmr1 exclusively from migrating neuroblasts using electroporation-mediated RNA interference method (MiRFmr1 KD). These impressive approaches show that neuroblasts tangential migration is impaired in Fmr1-null mice RMS and these defects are mostly recapitulated in the MiRFmr1neuroblasts. This nicely supports the idea that FMRP have a cell autonomous function in tangentially migrating neuroblasts. Authors also confirm that FMRP mRNA target Microtubule Associated Protein 1B (MAP1B) is overexpressed in the Fmr1-null mice RMS. They successfully use electroporation-mediated RNA interference method to silence Map1b in the Fmr1-null mice neuroblasts. This discreet and elaborate experiment rescues most of the migratory defects observed both in Fmr1-null and MiRFmr1neuroblasts. Altogether, these results strongly suggest that FMRP-MAP1B axis has an important role in regulation of the neuroblasts tangential migration in the RMS. Neurons move forward in cyclic saltatory manner which includes repeated steps of leading process extension, migration of the cell organelles and nuclear translocation. Authors reveal by analyzing the live-imaging data that FMRP-MAP1B axis is affecting movement of centrosome and nucleus during saltatory migration. An important part of the centrosome and nucleus movement is forces mediated by microtubule dynamics. Authors propose that FMRP regulate tangential migration via microtubule dynamics regulator MAP1B. This work provides valuable new information on regulation of the neuroblasts tangential saltatory migration. These findings also increase and improve our understanding of the issues involved in Fragile X Syndrome (FXS) disorders. The conclusions of this work are supported by the presented data.

The current version of the study has improved substantially. Authors have enhanced the material and methods section including a more detailed section on the neuronal migration analysis. This amendment is a very valuable addition and strengthens the interpretation of the results, analysis and conclusions. Authors also have strengthened and clarified their results providing a more profound analysis of the migration directionality between controls, Fmr1-null, MiRFmr1 KD and MiRMap1b KD neuroblasts. They have incorporated new results in the study which elaborate FMRP and MAP1B participation in microtubule organization during tangential migration. Authors show that FMRP-MAP1B axis act on microtubule cage surrounding the nucleus. Microtubule cage participate on proper nuclear movement during neuron migration. These results emphasize more the interplay between FMRP, MAP1B, and

the microtubule cytoskeleton. The authors have successfully expanded both the introduction and discussion sections of the manuscript.

https://doi.org/10.7554/eLife.88782.2.sa1

Reviewer #3 (Public Review):

Neuronal migration is one of the key processes for appropriate neuronal development. Defects in neuronal migration are associated with different brain disorders often accompanied by intellectual disabilities. Therefore, the study of the mechanisms involved in neuronal migration helps to understand the pathogenesis of some brain malformations and psychiatric disorders.

FMRP is an RNA-binding protein implicated in RNA metabolism regulation and mRNA local translation. FMRP loss of function causes fragile X syndrome (FXS), the most common form of inherited intellectual disability. Previous studies have shown the role of FMRP in the multipolar to bipolar transition during the radial migration in the cortex and its possible relation with periventricular heterotopia and altered synaptic communication in humans with FXS. However, the role of FMRP in neuronal tangential migration is largely unknown. In this manuscript, the authors aim to decipher the role of FMRP in the tangential migration of neuroblasts along the rostral migratory stream (RMS) in the postnatal brain. By extensive live-imaging analysis of migrating neuroblasts along the RMS, they demonstrate the requirement of FMRP for neuroblast migration and centrosomal movement. These migratory defects are cell-autonomous and mediated by the microtubule-associated protein Map1b.

Overall, the manuscript highlights the importance of FMRP in neuronal tangential migration. They performed an analysis of different aspects of migration such as nucleokinesis and cytokinesis in migrating neuroblasts from live-imaging videos. The authors have reinforced the results that associate defects in microtubule organization in Fmrp1 KO neurons and this rescue with the microtubule-associated protein Map1b. Overall, results concerning the role of Fmr1 in the tangential migration of neuroblasts are solid and convincing.

However, the work is still quite incomplete. My main concern is still what are the functional consequences of delay in neuroblast migration in the integration and function of OB interneurons and this relation with FXS pathophysiology. An anatomical examination of the RMS in the Fmr1KO mice is still missing.

https://doi.org/10.7554/eLife.88782.2.sa0

Author Response

The following is the authors' response to the original reviews.

We sincerely appreciate the constructive and insightful comments provided by the reviewer. Their valuable suggestions have been meticulously considered, leading to comprehensive modifications within the article.

In addition, we want to stress that we have implemented a significant additional modification by introducing a new figure (Fig. 6). This figure highlights the collaborative impact of FMRP and Map1B on the microtubular structure of migrating neurons. We firmly believe that this molecular elucidation of the migration phenotype constitutes a noteworthy addition to our work.

To Reviewer #1

We sincerely appreciate the constructive and insightful comments provided by the reviewer. Their valuable suggestions have been meticulously considered, leading to comprehensive modifications within the article.

In addition, we want to stress that we have implemented a significant additional modification by introducing a new figure (Fig. 6). This figure highlights the collaborative impact of FMRP and Map1B on the microtubular structure of migrating neurons. We firmly believe that this molecular elucidation of the migration phenotype constitutes a noteworthy addition to our work.

Public Review

(1) We have taken the necessary steps to enhance the material and methods section of our neuronal migration analysis. We apologize for any initial lack of detail, including the omission of information on sinuosity index and directionality radar. Regarding the query about speed, we want to clarify that it indeed encompasses the percentage of pausing time. The speed is calculated by dividing the total distance traveled by the cell by the total time it migrated.

(2) We would like to provide a clarification regarding the statistical analysis in our figures. The figures now represent the median, and the legend indicates the median along with the interquartile range. This approach is in line with the use of non-parametric analysis for variables that do not adhere to a normal distribution. Regrettably, in the previous version, there was an oversight in the figure legends where the mean, along with the standard error of the mean, was incorrectly stated instead of the intended representation of the median. We sincerely apologize for any confusion this may have caused. Moving forward, the corrected legend now accurately reflects the statistical measures used in the analysis.

The global Kruskal Wallis analysis, followed by Dunn's post hoc analysis, does indeed indicate that Fmr1 KD globally replicates the Fmr1-null phenotype. However, we concur with the reviewer's point regarding directionality, and we apologize for any lack of precision in the initial version. Upon further analysis, we have identified a significant difference in directionality (Fisher test $p < 0.001$). This more pronounced directionality defect in the KD could potentially be indicative of a lack of compensation, a factor that may not be at play in the Fmr1 null context. We appreciate the opportunity to address this issue and our revised version includes the necessary details to accurately convey these findings.

(3) We appreciate the referee's agreement with our perspective.

(4) In response to the recommendations from all referees, we have expanded both the introduction and discussion sections of our manuscript. The initial brevity of these sections was due to the short format we had initially chosen. We believe that these expansions contribute to a more comprehensive and nuanced presentation of our work, addressing the concerns raised by the referees.

The time stamp and scale bars were added.

The median versus mean issue is addressed above.

Figure numbering has been corrected (sorry for the mistake). The efficiency of CK is defined in the Mat and Met section.

> ***Recommendations for the authors***

The time stamp and scale bars were added.

The median versus mean issue is addressed above.

Figure numbering has been corrected (sorry for the mistake). The efficiency of CK is defined in the Mat and Met section.

> ***To Reviewer #2***
>
> ***Public review***

We express our gratitude to the referee for their positive appreciation of our work. We have carefully considered their suggestions and have modified the article accordingly.

In addition, as said to Referee #1, we want to stress that we have implemented a significant additional modification by introducing a new figure (Fig. 6). This figure highlights the collaborative impact of FMRP and Map1B on the microtubular structure of migrating neurons. We firmly believe that this molecular elucidation of the migration phenotype constitutes a noteworthy addition to our work.

(1) In light of the referee's recommendation, we conducted more resolutive staining of FMRP in SVZ neurons cultured in Matrigel, providing a more precise depiction of its subcellular localization (see Figure 1). Additionally, we have removed the sentence referring to growth cone staining, as it was not visibly present in cultured neurons. We appreciate the guidance from the referee in refining our study.

(2) We have also added a new figure 4 with better staining of MAP1B in the RMS as well as a more resolutive MAP1B staining in cultured neurons.

With all due respect, we maintain that the western blot experiments, conducted in three independent experiments, unequivocally support the conclusion of a 1.6X increase in MAP1B in the RMS of Fmr1null mutants, a trend observed in other systems.

In accordance with the referee's suggestion, we endeavored to quantify RMS immunostainings. Regrettably, the results proved inconclusive. This outcome is not entirely unexpected, as immunostainings are recognized for their inherent challenges in quantification. The additional complexity introduced by neonate perfusion further contributes to the notable interindividual variability observed.

(3) The efficiency of the two interfering RNAs is now documented in the text. Regarding the directionality radar, as highlighted for Ref 1 (public review, point #2), we acknowledge that, while Fmr1KD generally recapitulates the migratory phenotype of the Fmr1 mutants, more precise statistical analysis reveals differences in directionality, which is now documented. We apologize for the previous lack of precision.

(4) The suggested experiment of overexpression is interesting but we faced challenges in its execution. Attempts to overexpress MAP1B through intraventricular electroporation of a CMV-MAP1B plasmid resulted in the immobilization of transfected cells in the SVZ, hindering further analysis of migration. We hypothesize that this outcome may be attributed to a discrepancy in the actual dosage of MAP1B in the mutants.

Recommendations for the authors

(1) In light of the referee's recommendation, we conducted more resolutive staining of FMRP in SVZ neurons cultured in Matrigel, providing a more precise depiction of its subcellular localization (see Figure 1). Additionally, we have removed the sentence referring to growth cone staining, as it was not visibly present in cultured neurons. We appreciate the guidance from the referee in refining our study.

(2) We have also added a new figure 4 with better staining of MAP1B in the RMS as well as a more resolutive MAP1B staining in cultured neurons.

With all due respect, we maintain that the western blot experiments, conducted in three independent experiments, unequivocally support the conclusion of a 1.6X increase in MAP1B in the RMS of Fmr1null mutants, a trend observed in other systems.

In accordance with the referee's suggestion, we endeavored to quantify RMS immunostainings. Regrettably, the results proved inconclusive. This outcome is not entirely unexpected, as immunostainings are recognized for their inherent challenges in quantification. The additional complexity introduced by neonate perfusion further contributes to the notable interindividual variability observed.

(3) The efficiency of the two interfering RNAs is now documented in the text. Regarding the directionality radar, as highlighted for Ref 1 (public review, point #2), we acknowledge that, while Fmr1KD generally recapitulates the migratory phenotype of the Fmr1 mutants, more precise statistical analysis reveals differences in directionality, which is now documented. We apologize for the previous lack of precision.

(4) The suggested experiment of overexpression is interesting but we faced challenges in its execution. Attempts to overexpress MAP1B through intraventricular electroporation of a CMV-MAP1B plasmid resulted in the immobilization of transfected cells in the SVZ, hindering further analysis of migration. We hypothesize that this outcome may be attributed to a discrepancy in the actual dosage of MAP1B in the mutants.

(5) Concerning this point, and as mentioned above, we have incorporated a crucial piece of information into the manuscript, presented in Figure 6. The data reveal a severe disruption in the microtubular cage surrounding the nucleus of migrating neurons in Fmr1 mutants, a phenomenon rescued by MAP1B knock-down. Based on these findings, we believe we can confidently conclude that the microtubule-dependent functions of MAP1B play a role in the migratory phenotype of Fmr1 mutants. We consider this experiment to be a highly valuable addition to our work, shedding light on the underlying molecular mechanisms.

To Reviewer #3

We thank the referee for their insightful comments and have taken their consideration with great considerations.

In addition and as said above, we want to stress that we have implemented a significant additional modification by introducing a new figure (Fig. 6). This figure highlights the collaborative impact of FMRP and Map1B on the microtubular structure of migrating neurons. We firmly believe that this molecular elucidation of the migration phenotype constitutes a noteworthy addition to our work.

With regard to the perceived 'incompleteness' of our work, we believe that the addition of Figure 6, illustrating the molecular underpinnings of the Fmr1 mutation on the microtubular

Public review

With regard to the perceived 'incompleteness' of our work, we believe that the addition of Figure 6, illustrating the molecular underpinnings of the Fmr1 mutation on the microtubular cytoskeleton and its rescue in the MAP1B KD, significantly enhances the completeness of our study.

In response to the comment on the introduction and discussion sections, we acknowledge that their brevity was due to the Short Format initially chosen. We have since expanded these sections, incorporating additional information about FMRP and MAP1B and their influences on migration.

Regarding the La Fata article, as highlighted in our discussion, it's important to note that while the study did not strongly indicate an impact on radial locomotion per se, drawing conclusive results is challenging due to the relatively low number of analyzed neurons. Consequently, we do not believe that it poses a challenge to our findings.

With respect to MAP1B overexpression, as previously mentioned in response to Ref #2, point 4, our attempts resulted in the inhibition of migration, potentially due to an overdosage of the protein.

In terms of anatomical consequences, as highlighted in our discussion, while our neurons experience a delay in migration, they eventually reach their destination. Although a delay in migration may not directly result in significant anatomical anomalies, we acknowledge that the timing of differentiation can be crucial. As noted by Bocchi et al. (2017), a delay in the timing of differentiation for neurons reaching their target could lead to notable functional consequences. In any case, we have tOned down any references to the implication for the pathology.

- The size of the figures has been modified
- The pausing time and sinuosity are now defined
- The centrin-RFP labeling was indeed too weak in the previous version, which we corrected. We apologize for this.
- Fig S3 has been revised to address concerns. Notably, the decision to present the two bands for Vinculin and MAP1B separately is intentional. The blot is cut to allow independent development due to the substantial difference in their development times. We believe this approach provides a more accurate representation of the data.
- The numbering of the figures has been corrected. Sorry for the initial mistake.
- The Mat and Meth section has been corrected. Please note that we did not use any culture insert in this study.
- The tittle has been modified
- Comments about the Map1B overexpression experiment are expressed above and in replies to ref #2.